IMMUNOINFORMATICS-AIDED DESIGN OF A MULTI-EPITOPE VACCINE AGAINST MPOX

M'ember Chagu¹, Malachy Ifeanyi Okeke²*

^{1,2}Department of Natural and Environmental Sciences, Biomedical Science Concentration, School of Arts and Sciences, American University of Nigeria, 98 Lamido Zubairu Way, PMB 2250 Yola, Adamawa State, Nigeria (member.chagu@aun.edu.ng¹, malachy.okeke@aun.edu.ng²)

Abstract

Mpox, previously called monkeypox is zoonotic disease caused by the Monkeypox virus. Recent global outbreaks in non-endemic countries demonstrated its significance as a threat to public health. Currently, there are no preventive therapies or vaccines which target Mpox specifically. Herein, we aim to identify immunodominant B and T cell epitopes from this virus and design subunit vaccines using a reverse vaccinology approach. Four target proteins, H3L, M1R, B6R and A35R which have crucial functions in the pathogenesis of this virus were selected for epitope mapping. Epitopes with high population coverage and promiscuity were shortlisted and fused with appropriate adjuvants and linkers. Four vaccine constructs were designed using epitopes from a single protein and one vaccine was formed using epitopes from the proteins in combination. All constructs were predicted to be antigenic and non-allergenic with suitable physicochemical parameters. The three-dimensional structure of all constructs was predicted via homology modelling. Molecular docking analysis revealed stable and energetically favourable interactions between cytotoxic T lymphocyte (CTL) epitopes and human leukocyte antigen (HLA) alleles and between vaccine constructs and toll-like receptors (TLRs) (2, 3 and 4). Although extensive experimental testing is required to show that the predicted strong binding with human immune receptors translates to robust immune responses against MPXV in situ, these results obtained show that the MPXV multiepitope vaccines (MEVs) have a strong binding affinity to human immune receptors.

Keywords: Mpox, Monkeypox virus, Multi-epitope vaccine, Immunoinformatics, Epitope, Molecular docking.

1. Introduction

Mpox (MPX) is an infectious viral disease which was first identified in humans in 1970 in the Democratic Republic of Congo. MPX was thought to be limited to Central and West Africa with sporadic cases reported outside of these geographic regions. However, the Mpox outbreak in 2022 represented a significant shift in the epidemiology of the disease with a drastic increase in the number of reported cases worldwide [1]. Most cases of MPXV infection are mild with symptoms such as vesiculopustular rashes, fever, headaches, muscle aches and swollen lymph nodes similar to smallpox. Lymphadenopathy, however, is a symptom unique to MPXV. In more severe case, complications such as septicaemia, encephalitis, bronchopneumonia and ocular infections resulting in permanent vision may develop from infection [2].

Monkeypox virus (MPXV), the etiological agent of MPX is an enveloped double stranded DNA virus of the genus *Orthopoxvirus* which is classified under the *Poxviridae* family. This *Orthopoxvirus* genus is also inclusive of other human pathogenic species such as *Cowpox virus* (CPXV), *Camelpox virus* (CMLV), *Vaccinia virus* (VACV) and *Variola virus* (VARV) which causes smallpox (SPX) disease. The genome of MPXV is 197 kb and contains 190 nonoverlapping ORFs with its double stranded DNA covalently joined at both terminals by palindromic hairpin loops [3]. The central coding region sequences (between ORFs C10L and A25R) of the genome highly conserved across all *Orthopoxviruses* contain genes that encode for essential viral replication and structural proteins [4]. This central region is flanked by less conserved inverted terminal repeats. Genes located in this terminal region of the genome encode for the virus—host interactions and are highly variable to accommodate a broad host range [5]. MPXV is phylogenetically divided into three distinct clades: Clade I (formerly known as the Central African/Congo Basin clade), Clade IIa and Clade IIb (formerly known as the West African clade) and these clades differ from one another epidemiologically and in symptomatology. Clade II demonstrates a case fatality rate of less than 1% and exhibits no

human-to-human transmission. Clade I, however, exhibits a case fatality rate of up to 10% with more severe symptoms and transmission from human to human [6]. MPXV can enter the host via a respiratory or dermal route. It is transmitted through direct contact with bodily fluids which include exposure to open lesions or respiratory droplets, some recent studies suggest contraction via sexual contact [7] [8].

The current therapeutic options used to prevent MPX are VACV vaccines- ACAM2000 and JYNNEOS with cross-protective reactivity against MPXV. ACAM2000 is second-generation live replicating smallpox vaccine [9]. While effective, this vaccine is associated with several adverse effects resulting from uncontrolled viral replication including myocarditis and pericarditis[10]. JYNNEOS is a third generation modified VACV (Ankara-Bavarian Nordic strain) virus. This vaccine is significantly safer than earlier generation vaccines with fewer side effects as it is non-replicating. However, there is a shortage of scientific evidence on the effectiveness of such vaccines against MPXV clade II which appears to be responsible for recent outbreaks [11]. Multiple-epitope vaccines (MEVs) against MPX may serve as targeted and safer alternative vaccine platform to live, recombinant or virus-vectored MPXV vaccines. Thus, the aim of this study is to develop MPX B and T cell epitope vaccines that have strong binding affinity to human immune receptors and may stimulate robust innate and acquired immunity.

2. Materials and Methods

2.1 Protein selection

The Monkeypox virus MPXV-M5312_HM12_Rivers reference genome (NCBI Accession: NC_063383) was retrieved from the Bacterial and Viral Bioinformatics Resource Centre (BV-BRC) in FASTA format. All proteins were analysed using Vaxijenv 2.0 (https://ddg-pharmfac.net/vaxijen/VaxiJen/VaxiJen.html), AllerTopv 2.1 (https://www.ddg-pharmfac.net/allertop_test) and ToxinPred (https://webs.iiitd.edu.in/raghava/toxinpred/protein.php) to determine the antigenicity, allergenicity and toxicity respectively.

2.2 Epitope prediction, evaluation and selection

The Cytotoxic T Lymphocytes (CTL) epitopes of selected proteins were predicted using the NETCTL server (NetCTL 1.2 - DTU Health Tech - Bioinformatic Services) at an epitope identification threshold 0.75 under A1 supertype. Peptides predicted to have a combined score above 0.75 were additionally tested for antigenicity and allergenicity. Peptides which were predicted to be non-allergenic and have an antigenicity score >0.4 were tested for MHC class I binding. The IEDB Next Gen T Cell Prediction - Class I tool (https://nextgen-tools.iedb.org/) which provides a reference set of 27 HLA (Human Leukocyte Alleles) class I alleles covering ~97% of the world's population was used to identify epitopes interacting with HLA class I alleles[12].

The IEDB MHC II-binding tool (https://nextgen-tools.iedb.org/) predicted Helper T Lymphocyte (HTL) epitopes by identifying peptides which possess a binding affinity to at least 3 out of 18 HLA class II alleles selected (HLA-DRB1*01:01, HLA-DRB1*03:01, HLA-DRB1*04:01, HLA-DRB1*07:01, HLA-DRB1*08:03, HLA-DRB1*10:01, HLA-DRB1*11:01, HLA-DRB1*12:01, HLA-DRB1*13:02, HLA-DRB1*14:01, HLA-DRB1*15:01, HLA-DRB1*09:01, HLA-DRB3*02:02, HLA-DRB3*01:01, HLA- DRB4*01:01, HLA-DRB5*01:01, HLA-DRB1*04:04, HLA-DRB1*04:05) which cover ~95% of the world. Epitopes for the vaccine construct were selected based on the lowest percentile ranking as lower percentile rankings reflect a higher binding affinity of epitopes to HLA alleles.

The ABCpred server (https://webs.iiitd.edu.in/raghava/abcpred/) which utilises Artificial Neural Network (ANN) to predict linear B cell epitopes was used. Only epitopes which scored above the cutoff of 0.8 were selected as vaccine construct candidates.

2.3 Docking of CTL epitopes with HLA class I alleles

3D models of epitopes were generated by PEP-FOLD 3 (<u>PEP-FOLD Peptide Structure Prediction Server</u>) and docked against HLA allele structures retrieved from the Protein Data Bank (PDB) using Cluspro. Molecular docking was carried out between the best CTL epitope from each protein and its corresponding HLA allele as predicted by IEDB Next Gen T Cell Prediction - Class I tool.

2.4 Construction of Multi-Epitope Vaccines and Physiochemical Analysis.

CTL, HTL and B cell epitopes were connected using AAY, GPGPG, and KK linkers respectively. The Onchocercavolvulus activation-associated secreted protein-1 (Ov-ASP-1) was selected to be the vaccine adjuvant for its function in eliciting antibodies and as an agonist for Toll-like receptors 2 and 4 [13]. The Pan DR-binding epitope (PADRE) sequence was incorporated in the construct as an adjuvant due to its ability to bind HLA class II receptors despite their extreme polymorphism [14]. Adjuvants were separated from epitopes using the EAAAK sequence at the N terminal of the amino acid sequence. The physiochemical properties of the vaccine constructs were predicted using Protparam (https://web.expasy.org/protparam/) and were evaluated based on the general vaccine physiochemical requirements. These requirements consist of a molecular weight between 30-70KDa, a theoretical PI > 7, half-life in E.coli >10hrs and an instability index <40.

2.5 Tertiary Structure Prediction, Refinement and Validation

The tertiary structures of the vaccine constructs were modelled using I-TASSER (zhanggroup.org). Structures from the Protein Data Bank with high sequence identity to the vaccine amino acid sequences were identified using fold recognition and used as templates. To improve the quality of the optimal crude predicted structures, refinement was carried out using GalaxyRefine (https://galaxy.seoklab.org/). The stereochemical quality of refined structures was validated by analysing the percentage of residues in allowed regions of Ramachandran plots generated by PDBsum (https://www.ebi.ac.uk/thornton-srv/databases/pdbsum/). ProSAweb (https://prosa.services.came.sbg.ac.at/prosa.php) was used to check whether the z-score of the refined structures was within the range of scores typically found for native proteins of similar size.

2.6 Molecular Docking of Constructed Vaccines against Toll-like Receptors 2, 3 and 4

Each vaccine construct was docked against Toll-like receptors 2, 3 and 4. 3D structures of the TLRs were obtained from the protein data bank (TLR2 PDB ID: 2z7x, TLR3 PDB ID: 1ziw, TLR4 PDB ID: 4g8a). The active site residues were identified and co-crystallized ligands were removed to prepare the receptors for docking using PyMOL. ClusPro 2.0 (https://cluspro.org/) was used to carry out docking in antibody mode. PRODIGY (https://rascar.science.uu.nl/prodigy/) was used to predict the binding energy and dissociation constant for each interaction. PDBsum was utilized to investigate molecular interactions.

3. Result

3.1 Protein selection

The UniProt (https://www.uniprot.org/uniprotkb) database retrieved 176 MPXV proteins for the MPXV-M5312_HM12_Rivers reference genome, vaccine targets were selected based several desirable properties. The antigenicity score of H3L, M1R, B6R, A35R surpassed the cutoff of 0.4 with predicted to scores of 0.4354, 0.6339, 0.5786 and 0.4976 respectively. All four proteins were also predicted to be both non-allergenic and non-toxic with amino acid lengths greater than 150 amino acids.

3.2 Epitope selection

The identification of an invading pathogen relies on a coordinated response by the adaptive immune system mediated by B- and T-cells to generate pathogen-specific memory. Cytotoxic T-cells or T-lymphocytes are critical for identifying antigenic peptides known as epitopes presented on MHC-I and directly lysing host cells that have been infected by intracellular pathogens such as MPXV. Helper T-cells or T-lymphocytes bind MHC-II molecules and secrete cytokines- chemical messengers which regulate the immune response by directing other immune cells to the site of infection [15]. B-lymphocytes or B-cells are primarily responsible for humoral adaptive immunity. B-cells recognize specific antigens through antigen receptors leading to their activation and secretion of neutralizing antibodies. They also contribute to long-term immunity through the formation of memory B cells (MBCs) [16]. Due to the essential roles played by B- and T-cells in identifying pathogens and generating long lasting immunity, epitopes from both lymphocytes must be included to construct an effective MEV. Following multiple layers of screening, 7 CTL epitopes (Table 1), 7 HTL epitopes (Table 2) and 8 linear B-cell epitopes (Table 3) were selected.

3.3 Docking of CTL epitopes with HLA class I alleles

All selected epitopes had multiple binding alleles (Table 1). To determine the single best allele to proceed with molecular docking, only alleles with a population frequency >5, IC50<1000nM and median binding percentile <1 was selected. Based on these parameters, the three-dimensional structure of the H3L, M1R, B6R and A35R epitopes modelled by PEP-FOLD 3 were docked against HLA-B*15:0, HLA-B*35:0, HLA-A*11:01 and HLA-B*15:01 alleles respectively (Figure 1).

3.4 Construction of Multi-Epitope Vaccines and Physiochemical Analysis.

Five vaccine constructs were assembled, each including the Onchocerca volvulus activation-associated secreted protein-1 (Ov-ASP-1) and PADRE adjuvants (Figure 2). Four single vaccine constructs containing only epitopes from a single protein (H3L, M1R, B6R, A35R) and one combinatorial construct containing epitopes from all the proteins. All single MEV constructs included five epitopes, the H3L construct comprised two HTL and B-cell epitopes with a single CTL epitope. The M1R, B6R, A35R constructs were identical with two CTL and B-cell epitopes and a single HTL epitope. The combinatorial MEV consisted of four CTL, HTL and B-cell epitopes.

The physiochemical properties the MEVs are presented in Table 4. Molecular weights of the constructs range from 35-50kDa, considered to be favourable for vaccine development. The theoretical pI for the constructs ranged from 9.17-9.43, all >7. The instability index for constructs lies far below the cutoff of 40, ranging from 17.22-24.28, this suggests a good resistance of the MEVs to degradation and proteolysis. The GRAVY index of each construct was negative, ranging from -0.384 to -0.537 indicating good solubility and hydrophilicity.

3.5 Tertiary Structure Prediction, Refinement and Validation

I-TASSER identified known protein structures from the protein data bank that resemble the query sequence via alignment. Models were constructed by combining fragments from these templates and building missing parts from scratch by ab initio folding [17]. Five models were generated by I-TASSER, models with the highest confidence (C) score were selected for each construct (Figure 3). Refinement was achieved by running a short molecular dynamics (MD) simulation to optimize side-chain packing and minimise the energy of the vaccine structures [18]. The improvements from the crude to refined vaccine constructs were validated by analysing the Ramachandran plots generated by PDBsum. A significant increase in the number of residues in the most favoured regions was recorded across all models with crude models averaging 65% and refined models averaging 83% (Table 5). The z-score of refined models as predicted by ProSA-web were more negative, scoring closer to high quality proteins of similar sizes.

3.6 Molecular Docking of Constructed Vaccines against Toll-like Receptors 2, 3 and 4

ClusPro 2.0 generated thirty clusters representing varying docking positions. In each docking case, the binding positions of clusters with significant sizes were evaluated to ensure TLR active site residues were interacting with the MEVs. The cluster sizes of selected docking positions ranged from 20 members (Combinatorial vaccine docked against TLR3) to 109 (B6R vaccine docked against TLR4). Docking positions submitted to PRODIGY showed that across all vaccine constructs, the binding energies range from -10.9 to -16.8 kcal/mol with dissociation constants between 4.5E-⁻¹³ and 1.0E⁻⁸. The low dissociation constants demonstrate strong binding affinity to the immune receptors. Consistent formation of multiple hydrogen bonds, salt bridges, and non-bonded contacts predicted by PDBSum across all complexes confirms stable and specific interactions between the designed vaccines and the immune receptors (Table 6) (Figure 4).

Table 1. Selected Cytotoxic T Lymphocytes (CTL) epitopes.

Residue number	Peptide sequence	MHC (I) binding affinity	Rescaled binding affinity	C-terminal cleavage affinity	Transport affinity	Combined prediction score	Allele
•			H3L				
							HLA-B*15:01
							HLA-B*35:01
							HLA-A*02:03
101	HLALWDSKF	0.1164	0.494	0.9354	2.612	0.7649	
			M1R				
							HLA-A*01:01
81							HLA-A*30:01

e-ISSN: 3027-0650

Vol. 3. Issue	1.654-666	October	30-Novermbe	r 1, 202

				v 01. 5, 1551	ne 1,054-000., Ot	lober 30-Nover	mber 1, 2025
	ATETYSGLT	0.3020	1.2821	0.0404	-0.5730	1.2595	HLA-A*02:06
							HLA-B*35:01
	VAGTGVQFY	0.2187	0.9284	0.4712	2.8270	1.1405	HLA-B*15:01
188							HLA-B*58:01
			B6R				
							HLA-A*11:01
							HLA-A*68:01
33	STETSFNDK	0.2126	0.9028	0.787	0.362	1.039	HLA-A*03:01
							HLA-A*02:06
							HLA-B*58:01
							HLA-A*02:03
171	CTANSWNVI	0.1745	0.741	0.4289	0.543	0.8324	
			A35R				
							HLA-B*15:01
							HLA-B*58:01
46	LSMITMSAF	0.1451	0.6162	0.1192	2.692	0.7687	HLA-B*35:01
							HLA-A*02:06
							HLA-A*01:01
70	ITDSAVAVA	0.1583	0.6721	0.7735	-0.556	0.7603	HLA-A*02:01

Table 2. Selected Helper T Lymphocytes (HTL) epitopes.

Start	End	Peptide sequence	Percentile Rank	MHC II Allele
		H3L		
234	248	AKYVEHDPRLVAEHR	0.07	HLA-DRB1*03:01
61	75	DYVFIQWTGGNIRDD	3	HLA-DRB1*09:01
,				
		M1R		
75	89	TYSGLTPEQKAYVPA	0.41	HLA-DRB1*14:01
		B6R		
49	63	DSGYHSLDPNAVCET	0.07	HLA-DRB1*01:01
		A35R	·	
113	127	HSDYKSFEDAKANCA	0.47	HLA-DRB1*04:01

Table 3. Selected linear B-cell epitopes.

Rank	Sequence	Start position	Score	
	H3L			
3	NDDPDHYKDYVFIQWT	53	0.87	
5	YVFIQWTGGNIRDDDK	62	0.85	
	M1R			
2	IEIGNFYIRQNHGCNI	36	0.89	
3	DECYGAPGSPTNLEFI	134	0.88	
	B6R			
6	PTCVRSNEEFDPVDDG	235	0.88	
9	KLTSTETSFNDKQKVT	30	0.83	
	A35R			
1	VVSSTTQYDHKESCNG	87	0.9	

160

2

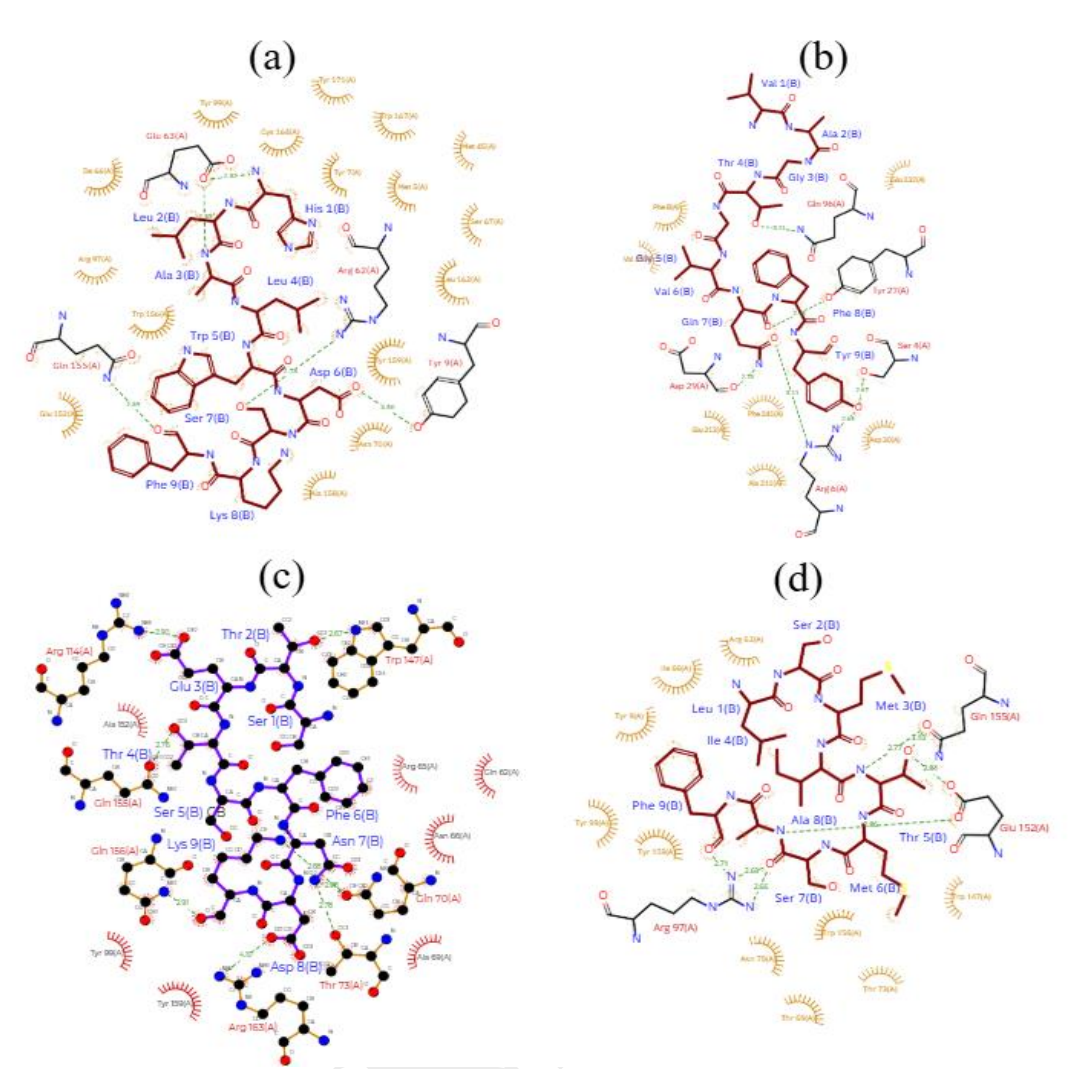


Figure 1. Docking of CTL epitopes against HLA alleles. (a) H3L epitope docking interactions with HLA-B*15:01. (b) M1R epitope docking interactions with HLA-B*35:01. (c) B6R epitope docking interactions with HLA-A*11:0. (d) A35R epitope docking interactions with HLA-B*15:01.

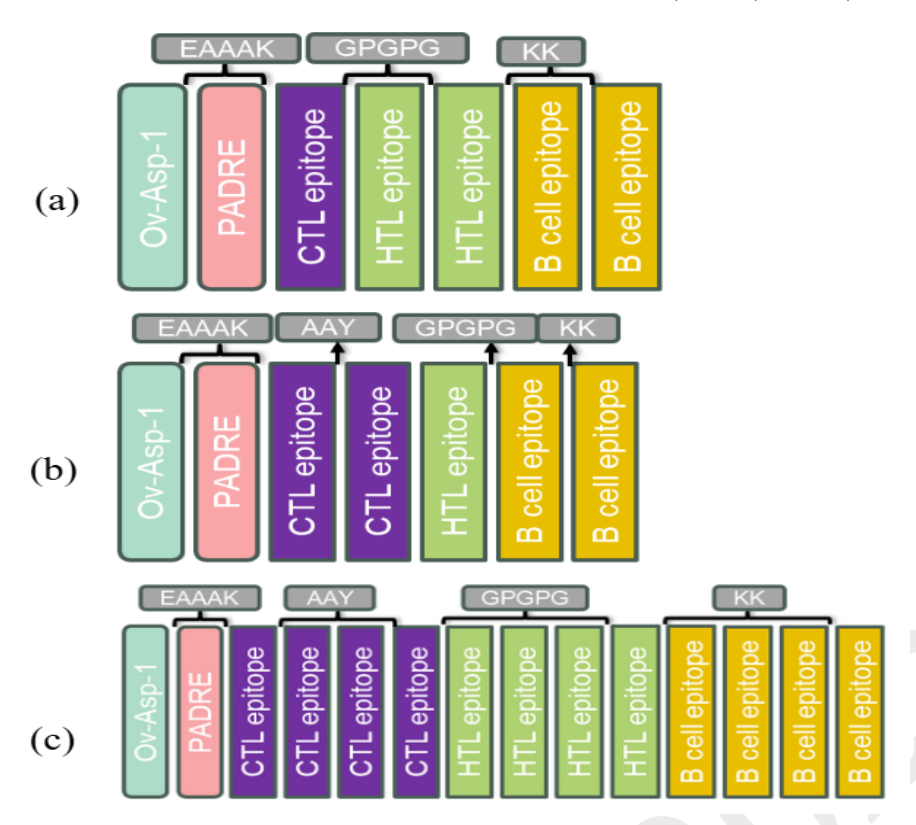


Figure 2. Topological representation of the final vaccine constructs. (a) H3L vaccine construct. (b) M1R, B6R, A35R vaccine constructs. (c) Combinatorial vaccine constructs.

Table 4. Physiochemical parameters of vaccine constructs.

Vaccine construct	Molecular Weight (kDa)	Theoretical pI	Instability Index	Aliphatic Index	GRAVY (Grand Average of Hydropathicity)
H3L	36652.95	9.40	17.22	68.11	-0.537
M1R	35151.38	9.43	24.28	69.13	-0.384
A35R	35129.19	9.35	22.16	66.40	-0.430
B6R	35289.26	9.28	20.49	63.94	-0.524
Combinatorial	50618 40	9 17	24 18	62.48	-0.495

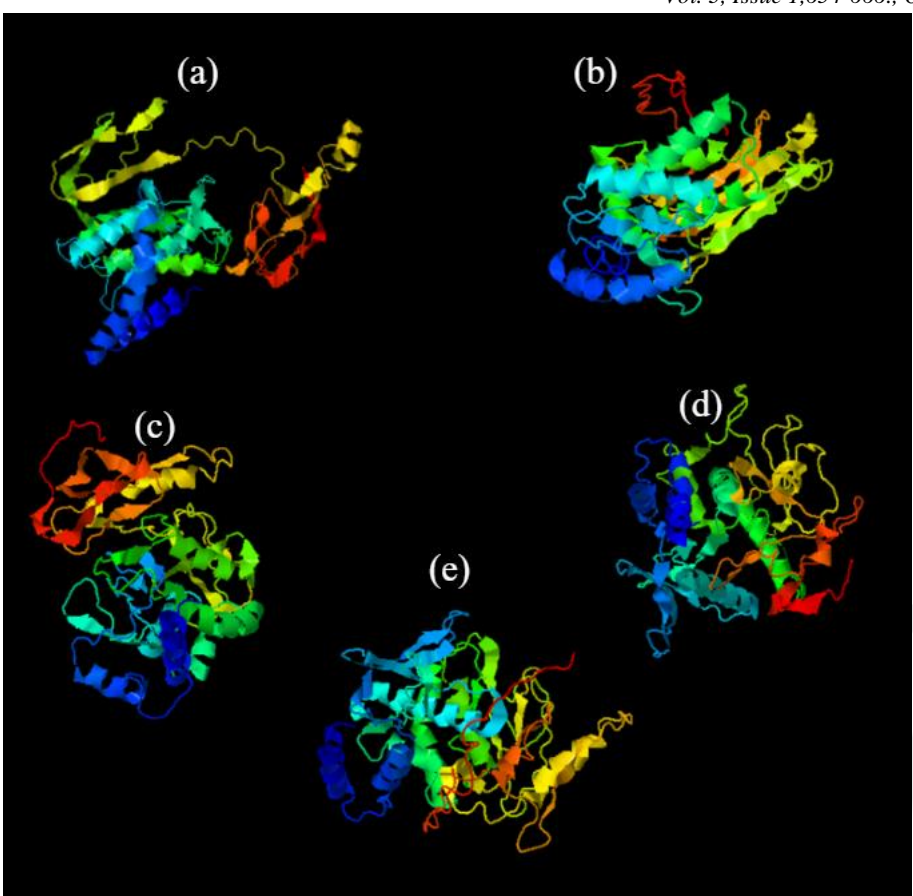


Figure 3. I-TASSER generated 3D structures of final vaccine constructs. (a) H3L model. (b) M1R model. (c) B6R model. model. (d) A35R model. (e) Combinatorial model.

Table 5. Structural refinement and validation of final vaccine constructs.

	Ramachandran plot fav	roured regions (%)	Z-score			
	Pre-refinement	Post-	Pre-refinement	Post-refinement		
		refinement				
H3L	65.0	80.9	-6.49	-6.68		
M1R	69.3	85.2	-6.36	-6.89		
B6R	67.5	84.8	-6.80	-7.43		
A35R	64.1	81.5	-5.98	-6.28		
Combinatorial	58.4	82.6	-2.73	-3.06		

Table 6. Docking interactions between vaccine constructs and TLRS 2, 3 and 4.

Interaction	Centre	Lowest	Cluster	Binding	Dissociation	Hydrogen	Salt	Non-
		energy	size	Energy	Constant	bonds	bridges	bonded
				$\Delta G(\text{kcal/mol})$	Kd(M)			contacts
H3L/TLR2	-358.2	-472.4	45	-16.4	9.6E-13	15	5	86
H3L/TLR3	-331.6	-511.7	58	-14.2	3.6E-11	17	7	148
H3L/TLR4	-371.8	-474.5	31	-15.5	4.2E-12	24	4	148
M1R/TLR2	-312.7	-366.9	46	-13.4	1.5E-10	10	-	79
M1R/TLR3	-319.9	-389.4	56	-12.1	1.4E-09	11	1	118
M1R/TLR4	-319.4	-395.2	50	-11.1	6.9E-09	16	3	134
B6R/TLR2	-308.1	-397.1	45	-10.9	1.0E-08	11	4	98
B6R/TLR3	-325.5	-389.7	24	-15.0	1.1E-11	29	7	222
B6R/TLR4	-356.6	-465.1	109	-11.2	6.2E-09	19	5	138
A35R/TLR2	-314.5	-345.4	22	-13.5	1.2E-10	19	8	133
A35R/TLR3	-404.5	-408.8	45	-13.3	1.6E-10	24	9	188
A35R/TLR4	-337.7	-368.9	33	-14.5	2.1E-11	15	5	136
Comb/TLR2	-413.9	-413.9	33	-13.5	1.2E-10	13	8	116
Comb/TLR3	-399.2	-412.5	20	-11.9	1.7E-09	18	6	156
Comb/TLR4	-363.7	-439.8	28	-16.8	4.5E-13	16	6	125

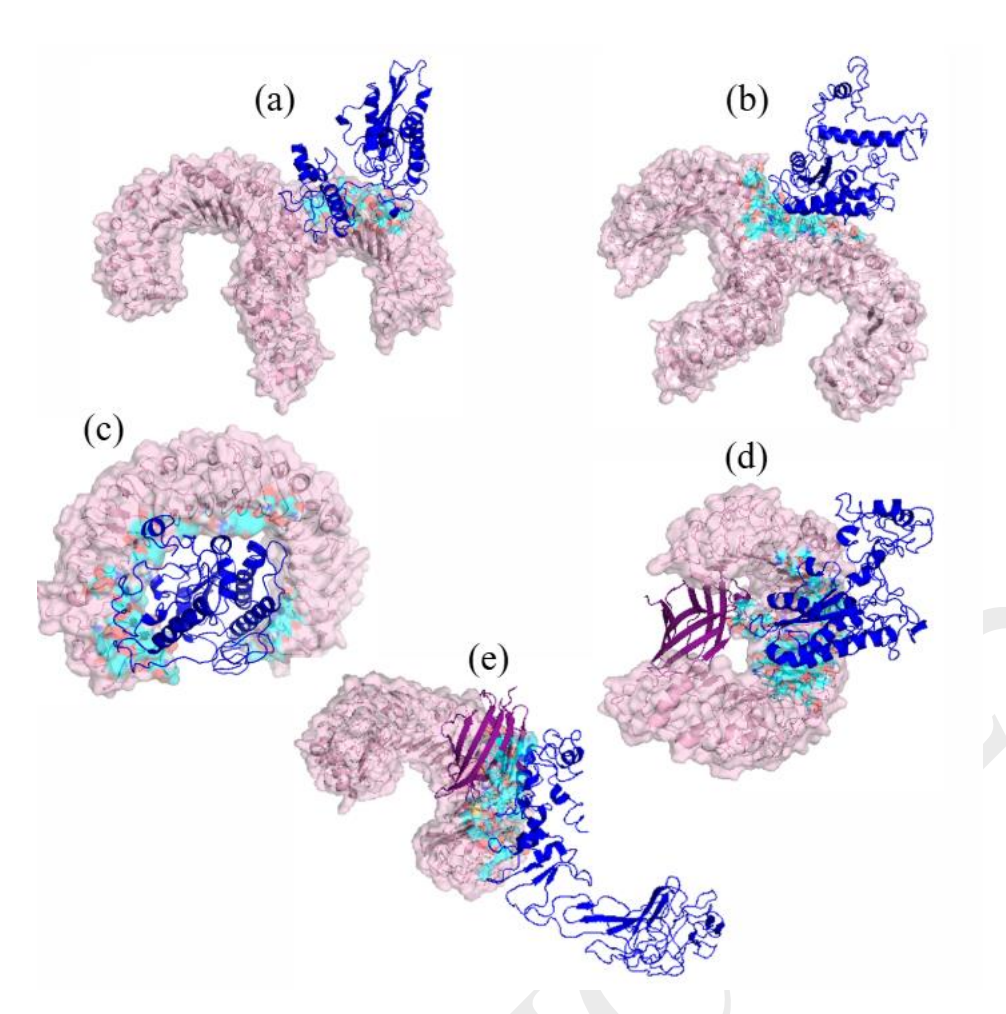


Figure 4. Best performing docked complexes with vaccines represented by blue and TLRs represented by pink. (a) H3L vaccine docked against TLR2. (b) M1R vaccine docked against TLR2. (c) B6R vaccine docked against TLR3. (d) A35R vaccine docked against TLR4. (e) Combinatorial vaccine docked against TLR 4.

4. Discussion

This study successfully employed a comprehensive immunoinformatics pipeline to design and evaluate five novel multi-epitope vaccine constructs against MPXV. The central finding of this research is the robust *in silico* evidence demonstrating the high affinity and stable binding of these constructs with critical immune receptors. Specifically, molecular docking analyses revealed that all designed vaccines, including the four single-protein constructs (H3L, M1R, B6R, A35R) and the combinatorial construct form energetically favourable complexes with Toll-like Receptors 2, 3, and 4. Predicted CTL epitopes also exhibit good molecular interactions with an array of MHC-I alleles. The exceptionally low binding energies (e.g., H3L/TLR2: $\Delta G = -16.4$ kcal/mol, Kd = $9.6E^{-13}$; Comb/TLR4: $\Delta G = -16.8$ kcal/mol, Kd = $4.5E^{-13}$) and the high number of hydrogen bonds, salt bridges, and non-bonded contacts indicate strong and specific interactions. This suggests that the vaccines are capable of effectively engaging both the innate immune system (via TLR activation) and the adaptive immune system (via MHC-I and MHC-II presentation), thereby potentially eliciting a potent humoral and cellular immune response against a MPXV infection.

Despite the promising computational results, this study is not without limitations, a primary one being the challenge encountered during the homology modelling phase. The prediction of the three-dimensional structures of the vaccine constructs via I-TASSER was complicated by

the lack of highly similar template structures in the protein databank. This is inherent to the design of novel multi-epitope vaccines, which are chimeric proteins with artificial linkers and adjuvants, making them unique sequences without direct structural homologs. This was reflected in the initial Ramachandran plot favoured regions, which for some constructs were far below 70% pre-refinement. Although refinement significantly improved these values (all above 80%), the reliance on threading and ab initio modelling methods introduces a degree of uncertainty in the predicted tertiary structures. Overall, we have shown that the multiepitope vaccine constructs binds strongly to human immune receptors and thus are good candidates for further evaluation of its vaccine potential against Mpox. Future work is geared to evaluating the thermodynamic stability of the vaccine constructs, its cloning and expressions as well as evaluating the immune responses in relevant *in silico*, *in vitro* and *in vivo* experimental models.

Author Contributions

M'ember Chagu: Methodology – investigation, data acquisition and interpretation; Writing - original draft preparation, Malachy Ifeanyi Okeke: conceptualization, supervision and project management; Methodology – Data Interpretation, Writing – review and editing.

Funding

The research received no external funding.

Conflict of Interest

The authors declare no conflict of interests.

References

- [1] P. Singh *et al.*, 'The resurgence of monkeypox: Epidemiology, clinical features, and public health implications in the post-smallpox eradication era', *New Microbes New Infect.*, vol. 62, p. 101487, Dec. 2024, doi: 10.1016/j.nmni.2024.101487.
- [2] I. K. Damon, 'Status of human monkeypox: clinical disease, epidemiology and research', *Vaccine*, vol. 29, pp. D54–D59, Dec. 2011, doi: 10.1016/j.vaccine.2011.04.014.
- [3] S. N. Shchelkunov *et al.*, 'Human monkeypox and smallpox viruses: genomic comparison', *Febs Lett.*, vol. 509, no. 1, pp. 66–70, Nov. 2001, doi: 10.1016/S0014-5793(01)03144-1.
- [4] S. N. Shchelkunov *et al.*, 'Analysis of the Monkeypox Virus Genome', *Virology*, vol. 297, no. 2, pp. 172–194, June 2002, doi: 10.1006/viro.2002.1446.
- [5] N. Chakravarty *et al.*, 'Mpox Virus and its ocular surface manifestations', *Ocul. Surf.*, vol. 34, pp. 108–121, Oct. 2024, doi: 10.1016/j.jtos.2024.07.001.
- [6] J. L. Americo, P. L. Earl, and B. Moss, 'Virulence differences of mpox (monkeypox) virus clades I, IIa, and IIb.1 in a small animal model', *Proc. Natl. Acad. Sci. U. S. A.*, vol. 120, no. 8, p. e2220415120, doi: 10.1073/pnas.2220415120.
- [7] L. D. Nolen *et al.*, 'Extended Human-to-Human Transmission during a Monkeypox Outbreak in the Democratic Republic of the Congo', *Emerg. Infect. Dis.*, vol. 22, no. 6, pp. 1014–1021, June 2016, doi: 10.3201/eid2206.150579.
- [8] A. Antinori *et al.*, 'Epidemiological, clinical and virological characteristics of four cases of monkeypox support transmission through sexual contact, Italy, May 2022', *Eurosurveillance*, vol. 27, no. 22, p. 2200421, June 2022, doi: 10.2807/1560-7917.ES.2022.27.22.2200421.
- [9] M. F. Gruber, 'Current status of monkeypox vaccines', *Npj Vaccines*, vol. 7, no. 1, p. 94, Aug. 2022, doi: 10.1038/s41541-022-00527-4.
- [10] G. A. Poland, R. B. Kennedy, and P. K. Tosh, 'Prevention of monkeypox with vaccines: a rapid review', *Lancet Infect. Dis.*, vol. 22, no. 12, pp. e349–e358, Dec. 2022, doi: 10.1016/S1473-3099(22)00574-6.

- [11] S. F. Ahmed, M. S. Sohail, A. A. Quadeer, and M. R. McKay, 'Vaccinia-Virus-Based Vaccines Are Expected to Elicit Highly Cross-Reactive Immunity to the 2022 Monkeypox Virus', *Viruses*, vol. 14, no. 9, p. 1960, Sept. 2022, doi: 10.3390/v14091960.
- [12] D. Weiskopf *et al.*, 'Comprehensive analysis of dengue virus-specific responses supports an HLA-linked protective role for CD8+ T cells', *Proc. Natl. Acad. Sci. U. S. A.*, vol. 110, no. 22, pp. E2046-2053, May 2013, doi: 10.1073/pnas.1305227110.
- [13] W. Xiao *et al.*, 'Evaluation of recombinant Onchocerca volvulus activation associated protein-1 (ASP-1) as a potent Th1-biased adjuvant with a panel of protein or peptide-based antigens and commercial inactivated vaccines', *Vaccine*, vol. 26, no. 39, pp. 5022–5029, Sept. 2008, doi: 10.1016/j.vaccine.2008.07.028.
- [14] D. Rosa, 'The pan HLA DR-binding epitope improves adjuvant-assisted immunization with a recombinant protein containing a malaria vaccine candidate', *Immunol. Lett.*, vol. 92, no. 3, pp. 259–268, Apr. 2004, doi: 10.1016/j.imlet.2004.01.006.
- [15] R. Wang *et al.*, 'The interaction of innate immune and adaptive immune system', *MedComm*, vol. 5, no. 10, p. e714, 2024, doi: 10.1002/mco2.714.
- [16] J. L. Sanchez-Trincado, M. Gomez-Perosanz, and P. A. Reche, 'Fundamentals and Methods for T- and B-Cell Epitope Prediction', *J. Immunol. Res.*, vol. 2017, p. 2680160, 2017, doi: 10.1155/2017/2680160.
- [17] S. Wu, J. Skolnick, and Y. Zhang, 'Ab initio modeling of small proteins by iterative TASSER simulations', *BMC Biol.*, vol. 5, p. 17, May 2007, doi: 10.1186/1741-7007-5-17.
- [18] L. Heo, H. Park, and C. Seok, 'GalaxyRefine: protein structure refinement driven by side-chain repacking', *Nucleic Acids Res.*, vol. 41, no. Web Server issue, pp. W384–W388, July 2013, doi: 10.1093/nar/gkt458.